

# Introduction of an Electromagnetism Module in LS-DYNA for Coupled Mechanical Thermal Electromagnetic Simulations

P. L'Eplattenier, G. Cook, C. Ashcraft

LSTC, 7374 Las Positas Road, Livermore, CA 94551, USA

## Abstract

*A new electromagnetism module is being developed in LS-DYNA for coupled mechanical/thermal/electromagnetic simulations. One of the main applications of this module is Electromagnetic Metal Forming. The electromagnetic fields are solved using a Finite Element Method for the conductors coupled with a Boundary Element Method for the surrounding air/insulators. Both methods use elements based on discrete differential forms for improved accuracy. The physics, numerical methods and capabilities of this new module are presented in detail as well as its coupling with the mechanical and thermal solvers of LS-DYNA. This module is then illustrated on an Electromagnetic Metal Forming case.*

## Keywords

Modelling, Finite Element Method (FEM), Boundary Element Method (BEM)

## 1 Introduction

LS-DYNA is a highly advanced general-purpose nonlinear finite element program that is capable of simulating complex real world problems. The distributed memory solver provides very short turn-around times on Unix, Linux and Windows clusters. The major development goal of Livermore Software Technology Corporation (LSTC) is to provide within LS-DYNA capabilities to seamlessly solve problems that require multi-physics, multiple-stages, and multi-processing. LS-DYNA is suitable to investigate phenomena that involve large deformations, sophisticated material models and complex contact conditions [1]. LS-DYNA allows running an analysis explicitly or implicitly and combining different disciplines such as coupled thermal analysis, fluid dynamics, fluid-structure interaction, SPH (smooth Particle Hydrodynamics), EFG (Element Free Galerkin). The analysis capabilities also include nonlinear dynamics, rigid body dynamics, quasi-static simulations, normal modes, eigenvalue analysis, Eulerian capabilities, ALE (Arbitrary

Lagrangian Eulerian), failure analysis, implicit spring back, adaptive re-meshing, 2D and 3D formulations. LSTC provides additional software packages for pre- and post-processing as well as for optimization. Metal forming is one of LS-DYNA's main applications, with capabilities that allow one to simulate rolling, extrusion, forging, casting, spinning, ironing, super-plastic forming, sheet metal stamping, profile rolling, deep drawing, hydro-forming, multi-stage processing, spring back, hemming.

An electromagnetism (EM) module is under development in LS-DYNA in order to perform coupled mechanical/thermal/electromagnetic simulations [2]. Electromagnetic Metal Forming (EMF) is the main application of this development, but other processes could be simulated, where magnetic pressure induces mechanical stress and deformations and/or the Joule effect induces a heating process: magnetic metal cutting, magnetic metal welding, very high magnetic pressure generation, rail-gun type apparatus, computation of the stresses and deformations in various coils, magnetic flux compression, induced heating and so forth. This module allows us to introduce some source electrical currents into solid conductors, and to compute the associated magnetic field, electric field, as well as induced currents. These fields are computed by solving the Maxwell equations in the eddy-current approximation. The Maxwell equations are solved using a Finite Element Method (FEM) [3] for the solid conductors coupled with a Boundary Element Method (BEM) [4] for the surrounding air (or insulators). Both the FEM and the BEM are based on discrete differential forms (Nedelec-like elements [5]).

In the first part, the EM module will be presented, the FEM part, the BEM part, and the coupling with external circuits. In a second part, the coupling of the EM module with the rest of LS-DYNA, and in particular with the mechanical and thermal modules will be presented. In the third part, one EMF example is presented.

## 2 Presentation of the Electromagnetism module

### 2.1 Scalar Potential and Modified Vector Potential Formulation

Let  $\Omega$  be a set of multiply connected conducting regions. The surrounding insulator exterior regions will be called  $\Omega_e$ . The boundary between  $\Omega$  and  $\Omega_e$  is called  $\Gamma$ , and the (artificial) boundary on  $\Omega$  at the end of the meshing region (hence where the conductors are connected to an external circuit) is called  $\Gamma_c$ . In the following, we will denote  $\vec{n}$  as the outward normal to surfaces  $\Gamma$  or  $\Gamma_c$ . The electrical conductivity, permeability and permittivity are called  $\sigma$ ,  $\mu$  and  $\varepsilon$  respectively. In  $\Omega_e$ , we have  $\sigma = 0$  and  $\mu = \mu_0$ .

The Maxwell equations read:

$$\vec{\nabla} \times \vec{E} = -\frac{\partial \vec{B}}{\partial t} \quad (1)$$

$$\vec{\nabla} \times \frac{\vec{B}}{\mu} = \vec{j} + \varepsilon \frac{\partial \vec{E}}{\partial t} \quad (2)$$

$$\vec{\nabla} \cdot \vec{B} = 0 \quad (3)$$

$$\vec{\nabla} \cdot \varepsilon \vec{E} = 0 \quad (4)$$

$$\nabla \cdot \vec{j} = 0 \quad (5)$$

$$\vec{j} = \sigma \vec{E} + \vec{j}_s \quad (6)$$

Where  $\vec{E}$  is the electric field,  $\vec{B}$  the magnetic flux density,  $\vec{j}$  the total current density, and  $\vec{j}_s$  is a source current density.

We consider good enough conductors with low frequency varying fields such that the condition  $\varepsilon \frac{\partial \vec{E}}{\partial t} \ll \sigma \vec{E}$  is satisfied. This is called the low frequency or eddy-current approximation, and is very well satisfied in EMF experiments. We thus neglect the second term of the right hand side of equation (2). The divergence condition (3) allows writing  $\vec{B}$  as  $\vec{B} = \vec{\nabla} \times \vec{A}$  where we introduced the magnetic vector potential  $\vec{A}$  [6]. Equation (1) then implies that the electric field is given by  $\vec{E} = -\vec{\nabla} \phi - \frac{\partial \vec{A}}{\partial t}$  where  $\phi$  is the electric scalar potential. We use the Gauge condition  $\nabla \cdot \sigma \vec{A} = 0$  which allows a separation of the vector potential from the scalar potential in the equations. The Maxwell equations in terms of the 2 potentials then read:

$$\nabla \cdot \sigma \vec{\nabla} \phi = 0 \quad (7)$$

$$\sigma \frac{\partial \vec{A}}{\partial t} + \vec{\nabla} \times \frac{1}{\mu} \vec{\nabla} \times \vec{A} + \sigma \vec{\nabla} \phi = \vec{j}_s \quad (8)$$

With the boundary conditions:

$$\vec{n} \cdot \vec{\nabla} \phi = 0 \text{ on } \Gamma \quad (9)$$

$$\phi = \phi_c \text{ on } \Gamma_c \quad (10)$$

And

$$\vec{n} \times \vec{\nabla} \times \vec{A} = \vec{A}_e \text{ on } \Gamma \quad (11)$$

$$\vec{n} \times \vec{A} = \vec{A}_c \text{ on } \Gamma \quad (12)$$

Equation (10) allows the connection of the conductors to a voltage source and equation (12) to a current source, although we will show in the following that the connection with a current source can also be done through the BEM part of the system, allowing more flexibility when using conductors with non trivial topologies.

Once the potentials are computed, the electromagnetic fields are given by:

$$\vec{E} = -\vec{\nabla} \phi - \frac{\partial \vec{A}}{\partial t} \quad (13)$$

$$\vec{B} = \vec{\nabla} \times \vec{A} \quad (14)$$

$$\vec{j} = \sigma \vec{E} + \vec{j}_s \quad (15)$$

## 2.2 Finite Element Method

Equations (7) and (8) are solved in the conductors with a Finite Element Method using a library called “FEMSTER” developed at the Lawrence Livermore National Laboratories [7]. FEMSTER provides discrete numerical implementations of the concepts from differential forms (often referred as Nedelec elements)[8][9]. These include in particular the exterior derivatives gradient, curl and divergence, and also the div-grad, curl-curl and grad-div operators. FEMSTER provides four forms of basis functions, called 0-forms, 1-forms, 2-forms and 3-forms, defined on hexahedra, tetrahedra and prisms. At this time, only hexahedral elements are available in the EM module of LS-DYNA. The two other types will soon be available.

0-forms are continuous scalar basis functions that have a well defined gradient, the gradient of a 0-form being a 1-form. At first order, the degrees of freedom associated with a 0-form are the values of the scalar field at the nodes of the mesh. In our particular case, the 0-forms are used for the discretization of the scalar potential  $\phi$ .

1-forms are vector basis functions with continuous tangential components but discontinuous normal components. They have a well defined curl, the curl of a 1-form being a 2-form. At first order, the degrees of freedom of a 1-form are its line integrals along the edges of the mesh. They are used for the discretization of the electric field  $\vec{E}$ , the magnetic field  $\vec{H}$  and the vector potential  $\vec{A}$ .

2-forms are vector basis functions with continuous normal components across elements but discontinuous tangential components. They have a well defined divergence, the divergence of a 2-form being a 3-form. At first order, the degrees of freedom of a 2-form are its fluxes across all the facets of the mesh. They are used for the discretization of the magnetic flux density  $\vec{B}$ , and the current density  $\vec{j}$ .

Finally, the 3-forms are discontinuous scalar basis functions which can't be differentiated. Their degrees of freedom at first order are their integrals over the elements of the mesh.

These basis functions define spaces with an exact representation in the De-Rham sequence [7]. They also exactly satisfy numerically relations such as curl(grad)=0 or div(curl)=0, which are very important for conservation laws when solving the systems [10]. At first order, they allow one to solve partial differential equation at an integrated “Stokes theorem” level which proves to be very efficient and accurate, even on low density meshes, compared to using vector basis functions [10].

We will denote  $W^0$ ,  $W^1$ ,  $W^2$ , and  $W^3$  as the basis functions associated respectively with the 0, 1, 2, and 3-forms. Equation (7) is projected against 0-forms basis functions and equation (8) against 1-forms to give, after using the appropriate Greens vector identities and the boundary conditions (9) - (12) [10].

$$\int_{\Omega} \sigma \vec{\nabla} \phi \cdot \vec{\nabla} W^0 d\Omega = 0 \quad (16)$$

$$\int_{\Omega} \sigma \frac{\partial \vec{A}}{\partial t} \cdot \vec{W}^1 d\Omega + \int_{\Omega} \frac{1}{\mu} \vec{\nabla} \times \vec{A} \cdot \vec{\nabla} \times \vec{W}^1 d\Omega = - \int_{\Omega} \sigma \vec{\nabla} \phi \cdot \vec{W}^1 d\Omega + \frac{1}{\mu} \int_{\Gamma} [\vec{n} \times (\vec{\nabla} \times \vec{A})] \cdot \vec{W}^1 d\Gamma \quad (17)$$

Or equivalently after decomposing  $\bar{A}$  and  $\phi$  respectively on the 0-form and 1-form basis functions:

$$S^0(\sigma)\phi = 0 \quad (18)$$

$$M^1(\sigma)\frac{da}{dt} + S^1\left(\frac{1}{\mu}\right)a = -D^{01}(\sigma)\phi + Sa \quad (19)$$

Where we introduced the 0-form stiffness matrix  $S^0$ , the 1-form mass matrix  $M^1$ , the 1-form stiffness matrix  $S^1$  and the 0-1 form derivative matrix  $D^{01}$  [10]. The last term of equation (19) which involves the “outside matrix stiffness”  $S$  is computed using a Boundary Element Method.

### 2.3 Boundary Element Method

In order to compute  $Sa$ , an intermediate variable “surface current”  $\bar{k}$  is introduced. This surface current, defined on the boundary  $\Gamma$  is such that it produces the same vector potential (and thus  $\bar{B}$  field) in the exterior regions  $\Omega_e$  as the actual volume current flowing through the conductors [11]:

$$\bar{A}(x) = \frac{\mu_0}{4\pi} \int_{\Gamma} \frac{1}{|x-y|} \bar{k}(y) dy \quad \text{for all } x \in \Omega_e \text{ (and in particular for all } x \in \Gamma) \quad (20)$$

One then has:

$$[\bar{n} \times (\bar{\nabla} \times \bar{A})](x) = \frac{\mu_0}{2} \bar{k}(x) - \frac{\mu_0}{4\pi} \int_{\Gamma} \frac{1}{|x-y|^3} \bar{n} \times [(\bar{x}-\bar{y}) \times \bar{k}(y)] dy \quad \text{for } x \rightarrow x_0 \in \Gamma \quad (21)$$

When projecting these equations on the 1-forms basis functions for  $\bar{A}$  and the “twisted” 1-forms  $\bar{V}^1(x) = \bar{n} \times \bar{W}^1(x)$  for  $\bar{k}$  one gets the following matrix equations:

$$Pk = Da \quad (22)$$

$$Sa = Qk \equiv Q_S k + Q_D k \quad (23)$$

Where we introduced the BEM matrices

$$P_{i,j} = \frac{\mu_0}{4\pi} \iint_{\Gamma_x \Gamma_y} \frac{1}{|x-y|} \bar{V}_i^1(x) \bullet \bar{V}_j^1(y) d\Gamma_x d\Gamma_y, \quad D_{i,j} = \int_{\Gamma_x} \bar{V}_i^1(x) \bullet \bar{W}_j^1(x) d\Gamma_x \quad (24)$$

$$Q_{S_{i,j}} = \frac{1}{2} \int_{\Gamma_x} \bar{W}_i^1(x) \bullet \bar{V}_j^1(x) d\Gamma_x \quad (25a)$$

$$Q_{Di,j} = -\frac{1}{4\pi} \iint_{\Gamma_x \Gamma_y} \frac{1}{|x-y|^3} \bar{W}_i^1(x) \bullet \{\bar{n}_x \times [(\bar{x} - \bar{y}) \times \bar{V}_j^1(y)]\} d\Gamma_x d\Gamma_y \quad (25b)$$

The BEM method is very appealing since it does not need a mesh in the air surrounding the conductors. It thus avoids the meshing problems associated with the air, which can be significant for complicated conductor geometries. Also, for very small gaps between conductors, an air mesh could include a large number of very small and distorted elements. Even more importantly, the BEM avoid remeshing problems which arise when using an air mesh around moving conductors. Another advantage of the BEM is that it does not need the introduction of somewhat artificial infinite boundary conditions.

The main disadvantage of the BEM is that it generates full dense matrices like  $P$  and  $Q_D$  (24,25) in place of the sparse FEM matrices. This causes a-priori high memory requirement as well as longer CPU time to assemble the matrices and solve the linear systems. In order to limit the memory requirement, a domain decomposition is done on the BEM mesh, which splits the BEM matrices into sub-blocks. On the non-diagonal sub-blocks, a low rank approximation based on a rank revealing QR decomposition is performed. For sub-blocks corresponding to far away domains, the rank can be significantly smaller than the size of the sub-block, thus reducing the storage of the sub-block. We typically see reductions of by factors around 20 between the full dense matrix and the block matrix with low rank approximations. This low rank approximation also speeds up the matrix \* vector operation used intensively in the iterative method to solve the BEM system (22). This method still needs the assembly of the full sub-blocks before doing the low rank approximation, generating a time consuming assembly process. We currently are working on methods generating directly the low rank approximations of the sub-blocks.

The matrices  $P$  and  $Q_D$  (24-25b) become singular or nearly singular as  $x \rightarrow y$ , i.e. for self face integrals or integrals over neighbour faces with a common edge or a common node. Special methods have been included such as the ones described in [12] and [13]. These methods also allow more accurate integration on inhomogeneous faces, i.e. faces with large aspect ratio.

## 2.4 Divergence free surface current, connection with external circuits

The surface current  $\bar{k}$  is an equivalent boundary current to the actual volume current through the volume of the conductor and needs to be divergence free [11]. However, the twisted 1-forms basis functions  $\bar{V}^1$  do not satisfy this divergence free constraint. We first added it as an external constraint to the BEM system (22). More recently, we introduced the so called “loop-star” solenoidal-irrotational decomposition into the divergence free “loop” basis functions and the rest [14] [15]. At first order, a twisted 1-form associated with a surface edge represents a surface current flowing across the edge, i.e. with a unit surface flux across the edge and a zero surface flux across all the other surface edges. A loop basis function associated with a node can be seen as a linear combination with coefficients +1 or -1 of 1-forms associated with all the edges originating from the node, so that it represents a (divergence-free) current flowing around the node. One can show that when using first order basis functions, the loop basis function associated with all the nodes of the surface mesh (except one) form a complete basis of the divergence free

currents for topologically simple conductors [14]. For non simple conductors, i.e. containing holes or “handles”, a few extra non-local basis functions that we call “global currents” need to be added. For example in the case of a torus, two extra global currents need to be added, one corresponding to a current flowing in the toroidal direction, and one corresponding to a current flowing in the poloidal direction.

An algorithm based on the construction of a spanning tree on the surface mesh has been developed to automatically count the number of connected part, get their topologies by computing the “Betti numbers” [16], and in particular the number of global currents and then set the global current basis functions as linear combinations of the 1-form basis functions. The degrees of freedom associated with the global currents are used to impose current vs time constraints as a simple dirichlet constraint in the BEM system (one dirichlet constraint per imposed current). This method allows imposing currents in geometries where more traditional methods using dirichlet conditions on the FEM system (12) would require the introduction of cuts and/or multi-valued degrees of freedom. The above mentioned toroidal current in a torus is such an example. The use of loop and global current basis functions also gives an easy way to compute the self and mutual inductances, by solving BEM systems (22) with simple dirichlet constraints. In this manner, the conductors can be connected to a current source, a voltage source, or an R,L,C circuit.

## 2.5 Global integration scheme

The time integration of the FEM system (19) is done using an implicit backward euler method [10]:

$$[M^1(\sigma) + dtS^1(\frac{1}{\mu})]a^{t+1} = M^1(\sigma)a^t - dtD^{01}(\sigma)\varphi^{t+1} + dtSa^{t+1} \quad (26)$$

The BEM part of the right hand side  $dtSa^{t+1}$  also is implicit which proved to substantially improve the stability, thus allowing larger time steps. It is computed by solving the BEM system (22) (23) coupled with the FEM system (19) in an iterative way:

$$Pk_{n+1}^{t+1} = Da_n^{t+1} \quad (27)$$

$$[M^1(\sigma) + dtS^1(\frac{1}{\mu})]a_{n+1}^{t+1} = M^1(\sigma)a^t - dtD^{01}(\sigma)\varphi^{t+1} + dtQk_{n+1}^{t+1} \quad (28)$$

Until convergence on both  $k_n^{t+1}$  and  $a_n^{t+1}$ .

The FEM System (28) is solved using a direct solver. The BEM system (27) is solved using a pre-conditioned gradient method. The diagonal of the matrix has been used as a pre-conditioner. More recently, the diagonal block has been used instead [17], with significant reduction in the number of required iterations (typically by a factor between 1.5 and 3).

### 3 Coupling of the EM module with LS-DYNA

#### 3.1 Mechanical solver

Once the EM fields have been computed, the Lorentz force  $\vec{F} = \vec{j} \times \vec{B}$  is evaluated at the nodes and added to the mechanical solver. The mechanical and electromagnetic solvers each have their own time step. For a typical EMF simulation, the mechanical time step is about 10 times smaller than the electromagnetic one. At this time, the explicit mechanical solver of LS-DYNA is used when coupled with electromagnetism. The mechanical module computes the deformation of the conductors and the new geometry is used to compute the EM fields in a Lagrangian way.

Since the EM module is fully integrated in LS-DYNA, all the material models are available. LS-DYNA provides more than 130 metallic and non-metallic material models, many of them equipped with failure criteria, such as metals, plastics, visco-elastic, elasto-viscoplastic, glass, foam, elastomers and rubbers. Included also are strain rate and temperature dependant plasticity models such as Johnson-Cook [18], Zerilli-Armstrong [19] or Steinberg [20] models, which are particularly suitable for high speed forming simulations. Numerous equations of state are also available. These models can be used on an extensive element library with both under-integrated and fully-integrated element formulations. It includes different solid elements, thick shells, different 3- and 4-node shells and beams. At this time, the EM module is only available on solid elements. It should soon be extended to shells with appropriate treatment of the diffusion of the EM fields.

Finally, efficient contact algorithms have been developed for the mechanical solver, and over 25 different contact options are available. At this time, the contact purely is mechanical and thermal, not electromagnetic, i.e. a current can not flow from one conductor to another if they come in contact during the simulation. This will be added as well as an electromagnetic sliding contact capability, necessary for rail-gun applications.

#### 3.2 Thermal solver

The Joule heating term  $\frac{j^2}{\sigma\rho}$  is added to the thermal solver allowing to update the temperature. Several thermal models are available, isotropic, orthotropic, isotropic with phase change and so forth. The temperature can be used in turn in an electromagnetic equation of state to update the electromagnetic parameters, mainly the conductivity  $\sigma$ . At this time, a Burgess model [21] has been introduced.

#### 3.3 Input-output

Electromagnetic cards have been added to the standard LS-DYNA card list used to create the input deck. The LS-PREPOST software can be used to visualize the electromagnetic fields - current density, electric field, magnetic flux density, Lorentz force, joule heating, conductivity, surface current - in the same environment as the mechanical and thermal fields. These include fringe component, iso-contour, vector plots at a given time, and also time histories on chosen elements.



## 4 Presentation of a typical EMF case

We now present the electromagnetic forming of a 1 mm thick aluminum sheet on a conical die, with a 4.7 cm height and a 12 cm diameter. This experiment was performed at the Department of Mechanical Engineering, University Of Waterloo, Ontario, Canada [22]. The brass coil has a 10 cm diameter spiral shape with 7 turns, and a rectangular cross section 1 cm by 0.4 cm. A hexahedral 3D mesh was built for the coil and the workpiece, and shell elements were used for the die. The mesh is composed of 20736 elements for the coil, 32320 for the aluminium sheet, with 4 elements through the thickness, and 17220 shells for the die. This mesh generated 23056 BEM faces, and 23163 BEM nodes (and hence 23163 degrees of freedom in the BEM system). Figure 1 shows the mesh at initial time. The experimental current, rising to around 100 kA in 50  $\mu$ s was injected in the coil. Figure 2 shows the evolution of the shape of the plate as well as the current density in a cross section of the sheet. Figure 3 shows details of the rebounding of the sheet from the die. Figure 4 shows a comparison between the numerical and experimental final shape of the sheet. The final shape shows a good agreement. One can notice that the shape does not match the shape of the die, due to rebounding of the plate from the die and a non-uniform magnetic pressure on the sheet, with a significantly lower pressure at the centre. This low pressure area is reflected in the current density plots, and is due to the shape of the coil.

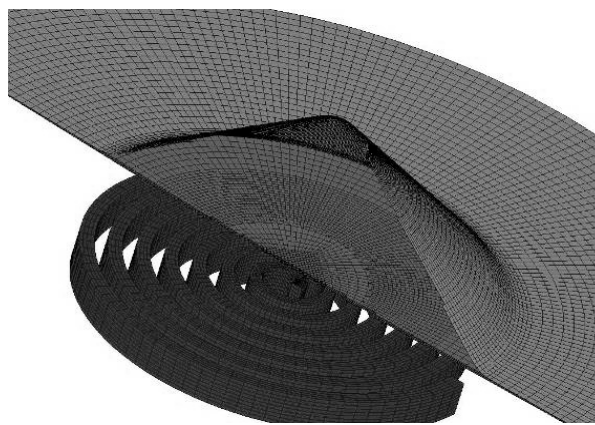


**Figure 1:** mesh of the EMF case. Only  $\frac{1}{2}$  of the sheet and die are represented.

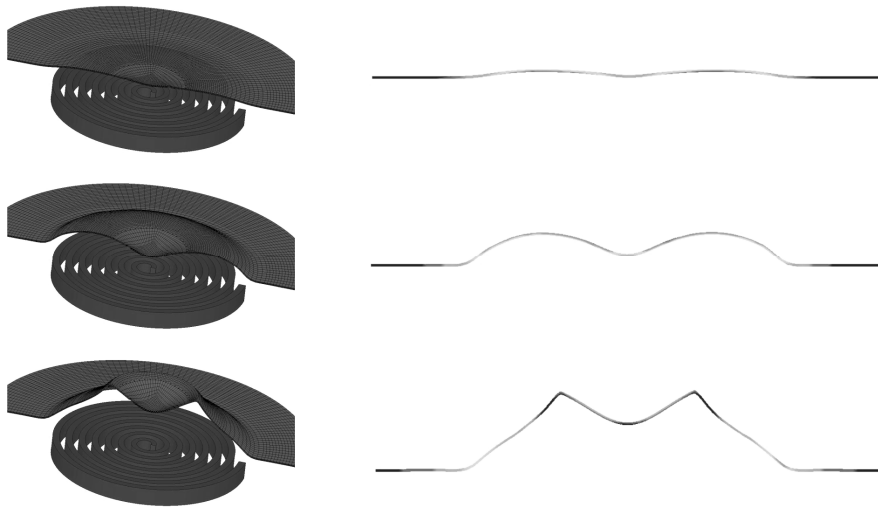


**Figure 2:** 3D shape of the sheet (left, only 1/2 of the sheet is represented), and current density in a cross section of the sheet (right) at 45 μs (top), 70 μs (middle) and 100 μs (bottom). The scale in the z-direction has been increased in the cross sections for better visibility.

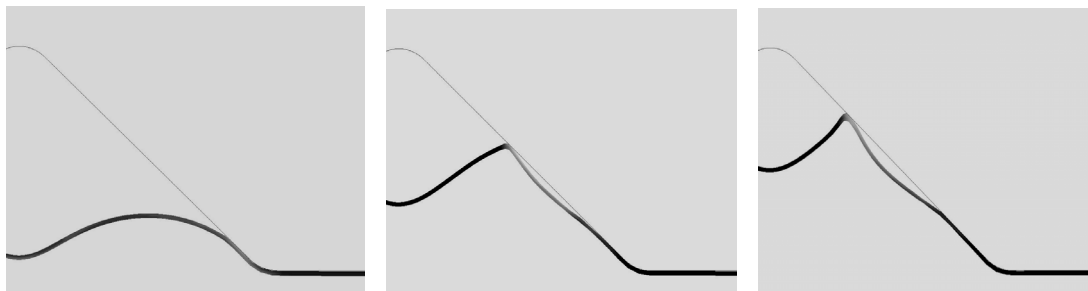


**Figure 3:** Detail of the rebounding of the sheet from the die: cross section of the sheet and die at 70 μs (left), 100 μs (middle) and 130 μs (right). Fringes are of plastic strain.

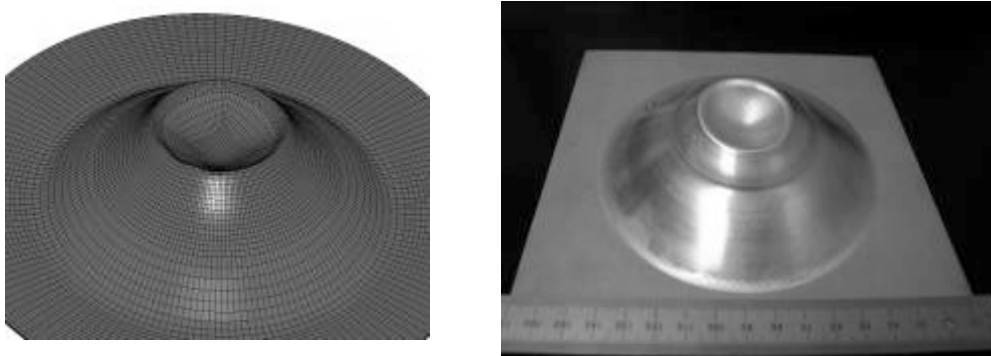


**Figure 4:** numerical (left) and experimental (right) final shape of the sheet.

## 5 Conclusion

The newly introduced Electromagnetism module of LS-DYNA was presented. The electromagnetic fields are computed by solving the Maxwell equations in the eddy-current approximation, using a Finite Element Method for the conductors coupled with a Boundary Element Method for the surrounding air and insulators. Loop basis functions are used to represent the BEM surface current, allowing to handle the divergence free constraint as well as easy connection with external circuits. A 2-dimensional ax symmetric version of the EM module is also available.

This module is integrated in the “Is980” version which should be released in late 2008. In the mean time, it is available as a “beta version”. The near-term future developments for the EM module include new BEM assembly methods, introduction of tetrahedral and wedge elements, development of an Massively Parallel Processor (MPP) version (the rest of LS-DYNA is currently available in MPP, but the EM module only is serial). The planned mid-term developments include the introduction of sliding contact capabilities for the electromagnetism, remeshing capabilities, extension to other solvers (magnetostatics and so forth). Longer-term developments could include the introduction of magnetic materials.

## Acknowledgment

The authors would like to thank M. Worswick and J.Imbert at the University of Waterloo, Ontario, Canada; G. Daehn, M. Seth Y. Zhang and A. Vivek at The Ohio State University, Columbus, OH, USA; G. Fenton at Applied Research Associates, Inc., Albuquerque, NM, USA; I. Ulacia at the University of Mondragon, Gipuzkoa, Spain; G. Le Blanc and G. Avrillaud at International Technologies for High Pulsed Power, Thegra, France; J. Thomas at The University of Michigan, Ann arbor, MI, USA; J. Shang at Hirotec America, Auburn Hills, MI, USA, and P.L. Hereil, P.Y. Chanal and A. Lefrancois at Centre d’Etudes De Gramat, Gramat, France, for very fruitful collaborations and for giving access to experimental or numerical data for comparisons and benchmarks.

## References

- [1] LS-DYNA Theory Manual, LSTC.
- [2] *P. L’Eplattenier; G. Cook, C. Ashcraft; M. Burger; A. Shapir; G. Daehn; M. Seith:* “Introduction of an Electromagnetism Module in LS-DYNA for Coupled Mechanical-Thermal-Electromagnetic Simulations”, 9th International LS-DYNA Users conference”, Dearborn, Michigan, June 2005.
- [3] *J. Jin:* “The Finite Element Method In Electromagnetics”, Wiley, 1993.
- [4] *J. Shen:* “Computational Electromagnetics Using Boundary Elements, Advances In Modelling Eddy Currents”, Topics in Engineering Vol 24, Series Eds: C.A. Brebbia and J.J. Connor, Southampton and Boston: Computational Mechanics Publications, 1995”.
- [5] *J.C. Nedelec:* “A New Family of Mixed Finite Elements in R<sup>3</sup>”, Num. Math, 50:57-81, 1986.

- [6] *O. Biro and K. Preis*: “On the use of the magnetic vector potential in the finite element analysis of three-dimensional eddy currents”, IEEE Transaction on Magnetics, 25(4)3145-3159,1989.
- [7] *P. Castillo, R. Rieben and D. White*: “FEMSTER: An object oriented class library of discrete differential forms”. In Proceedings of the 2003 IEEE International Antennas and Propagation Symposium, volume 2, pages 181-184, Columbus, Ohio, June 2003.
- [8] *Z. Ren and A. Razek*: “Computation of 3-D electromagnetic field using differential forms based elements and dual formulations”, International Journal of Numerical Modeling: Electronic Networks, Devices and Fields, Vol. 9, 81-98 (1996).
- [9] *R. Rieben*: “A Novel High Order Time Domain Vector Finite Element Method for the Simulation of Electromagnetic Devices”, Ph-D Thesis, University of California Davis, 2004.
- [10] *R. Rieben and D. White*: “Verification of high-order mixed finite element solution of transient magnetic diffusion problems”, IEEE Transaction on Magnetics, 42(1), 25-39, 2006.
- [11] *Z. Ren, A. Razek*: “New technique for solving three-dimensional multiply connected eddy-current problems”, IEE Proceedings, Vol. 137, Pt. A, No 3, May 1990.
- [12] *W. Wang and N. Atalla*: “A numerical algorithm for double surface integrals over quadrilaterals with a 1/r singularity”, Communications in Numerical Methods in Engineering, 13, 885-890 (1997).
- [13] *S. Sauter*: “Cubature techniques for 3-D Galerkin BEM”, Boundary Elements: Implementation and Analysis of Advanced Algorithms, W. Hackbusch, G. Wittum eds, NNNFM 54, Vieweg-Verlag (1996), 29-44.
- [14] *G. Vecchi*: “Loop-Star Decomposition of Basis Functions in the Discretization of the EFIE”, IEEE Transactions on Antennas and Propagation, Vol. 47, No 2, February 1999.
- [15] *J.L. Volakis, D.B. Davidson*: “Iterative-Solver Convergence for Loop-Star and Loop-Tree Decompositions in Method-of-Moments Solutions of the Electric-Field Integral Equation”, IEEE Antennas and Propagation, 46(3), 80-85, June 2004.
- [16] *A. Bossavit*: “Computational Electromagnetism”, Academic Press (Boston), 1998.
- [17] *K.E. Chen*: “On a class of preconditioning methods for dense linear systems from boundary elements”, SIAM J. Sci. Comput. 20(2), 684-698, 1998.
- [18] *G.R. Johnson, and W.H. Cook*: “Fracture Characteristics of Three Metals Subjected to Various Strains, Strain Rates, Temperatures and Pressures”, Engineering Fracture Mechanics, Vol 21, No 1, pp 31-48, 1985.
- [19] *F.J. Zerilli and R.W. Armstrong*: "Dislocation-mechanics-based constitutive relations for material dynamics calculations", J. Appl. Phys. 61(5), March 1987.
- [20] *D.J. Steinberg, S.G.Cochran, M.W.Guinan*: “A Constitutive Model for Metals Applicable at High-Strain Rate”, J. Appl. Phys. 51,1498 (1980)
- [21] *T.J. Burgess*: “Electrical resistivity model of metals”, 4<sup>th</sup> International Conference on Megagauss Magnetic-Field Generation and Related Topics, Santa Fe, NM, USA, 1986
- [22] *J. Imbert, M. Worswick, S. Winkler, S. Golovashchenko, V. Dmitriev*: “Analysis of the Increased Formability of Aluminum Alloy Sheet Formed Using Electromagnetic Forming”, Proceedings, SAE 2005, SAE Paper No. 2005-01-0082